J. Mech. Phys. Solids 169 (2022) 105090

Contents lists available at ScienceDirect

Journal of the Mechanics and Physics of Solids

journal homepage: www.elsevier.com/locate/jmps

Characterization of fracture toughness and damage zone of double network hydrogels

Yetong Jia [#], Zidi Zhou [#], Huilong Jiang, Zishun Liu [*]

International Center for Applied Mechanics, State Key Laboratory for Strength and Vibration of Mechanical Structures, School of Aerospace, Xi'an Jiaotong University, Xi'an, Shaanxi, 710049, China

ARTICLE INFO

Keywords:
Fracture toughness
Double network hydrogels
Damage zone
Feature size

ABSTRACT

Double-network (DN) hydrogels have received extensive attention owing to their excellent mechanical properties such as high fracture toughness. It is widely accepted that the toughening mechanism of DN gels is based on the mutual interaction of two contrasting interpenetrating networks. However, the quantitative interpretation of this toughening mechanism during fracture is still lacking; there are also some contradictions regarding the fracture toughness. In this study, we developed a quantitative framework to decompose the fracture toughness and feature size of the crack-tip field. Through extensive tearing tests with varying free widths of the tearing specimens, we propose an exponential function to describe the relationship between the apparent fracture energy and free width. Using the proposed function, the fracture energy and feature size of the dissipation zone were decomposed into their different components, and their quantitative values were obtained. Tearing tests were also conducted on prestretched DN gels, which showed that the intrinsic fracture energy is related to the historical deformation. Finally, we established an intrinsic fracture model with a clear physical meaning by considering the complex interactions between the two interpenetrating networks of DN gels. The model revealed the physical mechanism behind the dependence of the intrinsic fracture energy of DN gels on the historical loading. The contributions of the two interpenetrating networks of DN gels to the intrinsic fracture energy were quantitatively decomposed by the model, and the feature size of the intrinsic field was also obtained. The study reveals the physical inconsistencies in some opinions about DN gel fracture and resolves some paradoxes on the toughness of DN gels.

1. Introduction

In recent years, soft materials (e.g., hydrogels and elastomers) have drawn significant attention owing to their superior mechanical properties, such as large deformability (Liu et al., 2015), shape memory effect (Huang et al., 2020), and multistimuli response (Xu and Liu, 2020). With these unique properties, soft materials have numerous potential applications in various fields (Li et al., 2020; Liu et al., 2020; McCracken et al., 2020; Yang and Suo, 2018). However, emerging applications require the enhancement of the mechanical properties of soft materials, which facilitates the formation of double-network (DN) hydrogels (Gong, 2010; Gong et al., 2003). Compared with traditional single-network hydrogels, DN gels exhibit a high modulus and crack resistance because of their unique

* Corresponding author.
E-mail address: zishunliu@mail.xjtu.edu.cn (Z. Liu).
# These authors contributed equally to this work.

https://doi.org/10.1016/j.jmps.2022.105090
Received 9 July 2022; Received in revised form 5 September 2022; Accepted 28 September 2022

network structures. DN gels have two types of interpenetrating networks with contrasting structures: a rigid and brittle network with densely cross-linked short chains called the first network; and a soft and stretchable network with loosely cross-linked long chains called the second network. During deformation, the first network serves as sacrificial bonds to dissipate energy, whereas the second network maintains the integrity of the hydrogel. Although the structure of DN gels is relatively well understood (Fukao et al., 2020; Nakajima et al., 2013), a systematic understanding of the underlying toughening mechanisms of DN gels against crack propagation remains lacking owing to the complexity of the internal structures.

Fracture toughness is a mechanical property of materials that is commonly used to describe their resistance to crack propagation. For soft materials, the fracture toughness is often characterized by the fracture energy, which is defined as the energy required for a crack to propagate along a unit area. The fracture energy can be measured by various methods (Greensmith, 1963; Long and Hui, 2016; Rivlin, 1953), such as the pure shear test, single-edge notch test, and tearing test. For soft materials with large energy dissipation (e.g., DN gels), the apparent fracture energy Γ that is directly measured by the fracture test is normally decomposed into two parts: the intrinsic fracture energy Γ_0 and dissipated fracture energy Γ_d (Long et al., 2021; Long and Hui, 2016; Matsuda et al., 2021; Zhao, 2014)

$$\Gamma = \Gamma_0 + \Gamma_d \tag{1}$$

where Γ_0 is related to the chain scission at the crack tip (Lei et al., 2021), and Γ_d is the fracture energy due to mechanical dissipation (e.g., microstructural damage, viscoelasticity, plasticity) in the dissipation zone around the crack tip. The size of the dissipation zone ranges from micrometers to centimeters depending on the material (Long et al., 2021). According to recent studies, the fracture energy of DN gels ranges from 100 to 5000 $\mathrm{J/m^2}$ (Matsuda et al., 2020), while the dissipation zone is in the millimeter range (Long et al., 2021).

Over the last few years, the toughening mechanism of DN gels has been extensively investigated. Unlike brittle materials whose fracture energy is considered to be dominated by the intrinsic fracture energy, it is generally recognized that the fracture energy of DN gels is mostly contributed by the bulk energy dissipation (Liang et al., 2011; Long et al., 2021; Long and Hui, 2016; Yu et al., 2009). Damage to the first network results in the large energy dissipation of DN gels, while the intrinsic fracture energy Γ_0 is assumed to be very close to the toughness of the second network and much lower than the dissipated fracture energy Γ_d. The above studies suggest that $\Gamma_0 \approx \Gamma_{2nd-network} \ll \Gamma_d$, $\Gamma \approx \Gamma_d$.

To further clarify the toughening mechanism, efforts have been made to quantitatively determine the constituents of the fracture energy of DN gels. For the intrinsic fracture energy of soft materials, Zhao et al. (2021) reported that this could be measured by a fatigue test. During the fatigue test, the polymer chains of the first network were depleted in the crack-tip field, and only the chain scission of the second network contributed to the fracture energy during crack propagation. In this regard, the fatigue threshold is the intrinsic fracture energy. Another method to characterize the intrinsic fracture energy is by prestretching the DN gel to a certain degree before conducting the fracture tests (Matsuda et al., 2021; Zhang et al., 2015). The fracture energy of the prestretched specimen is considered to be close to the intrinsic fracture energy because most of the first-network strands were ruptured during the stretching process and the dissipative capacity was nearly consumed. However, it is worth mentioning that both the fatigue threshold of DN gels ($\sim 400\ \mathrm{J/m^2}$) (Zhang et al., 2018) and the fracture energy of prestretched DN gels ($\sim 700\ \mathrm{J/m^2}$) (Matsuda et al., 2021) are much larger than the fracture energy of the pure second network (PAAm, $\sim 100\ \mathrm{J/m^2}$). For the dissipated fracture energy of DN gels, a mechanochemical technique was recently developed for visualizing and quantifying the damage zone of DN gels. Through this technique, the damage distribution could be quantitatively represented as a fluorescence intensity map (Matsuda et al., 2020, 2021). By relating the fluorescence intensity to the tensile data, the dissipated energy density in the damage zone of DN gels could be quantitatively estimated. Using this mechanochemical method, the dissipated fracture energy was measured as $\sim 300\ \mathrm{J/m^2}$, which is considerably smaller than the apparent fracture energy of $\sim 900\ \mathrm{J/m^2}$ and of the same order of magnitude as the intrinsic fracture energy $\sim 500\ \mathrm{J/m^2}$. Based on these quantitative methods, it was realized that the intrinsic fracture energy of DN gels is much higher than the fracture energy of the pure second network, and even of the same order of magnitude as the dissipated fracture energy. These experimental results seem to contradict the previous understanding that $\Gamma_0 \approx \Gamma_{2nd-network} \ll \Gamma_d$, $\Gamma \approx \Gamma_d$, indicating that the underlying toughening mechanism of DN gels has yet to be fully understood and requires further study.

In this paper, we present a series of detailed fracture experiments and complementary theoretical modeling to elucidate several key issues regarding the paradoxes of the fracture energy of DN gels. We propose a set of quantitative methods to decompose the fracture energy and characteristic size of the crack-tip field of DN gels to reveal the underlying toughening mechanisms of DN gels and the deformation states in the crack-tip field. Experimental studies on the material synthesis and mechanical tests are described in Section 2. In Section 3, we present the experimental results of the tearing test, on the basis of which an exponential function is proposed to accurately describe the relationship between the fracture energy and free width. Then, the fracture energy and feature size of the dissipation zone are decomposed. The tearing test on prestretched DN gels demonstrates that both the apparent and intrinsic fracture energies are dependent on the historical deformation. In Section 4, an intrinsic fracture model is established to interpret the interaction between the two interpenetrating networks and their contribution to the intrinsic fracture energy. The feature size of the intrinsic field can also be obtained with this model. In Section 5, we discuss the feature sizes obtained in this study with two length scales that are widely used in the study of highly deformable soft materials. Compared with our feature sizes, these two length scales seem unsuitable for describing the crack-tip field of DN gels. Section 6 presents some concluding remarks.

2. Experimental investigations of DN gels

To explore the mechanical properties of the DN gel and its single-network hydrogel components during deformation and fracture,

we conducted the uniaxial tensile test, 180-degree peeling test, and tearing test.

2.1. Material synthesis

A two-step polymerization method was used for the DN gel (Gong et al., 2003). The 1-acrylamido-2-methylpropanesulfonic acid (AMPS; Aladdin) and acrylamide (AAm; Macklin) were used as the monomers of the first network (PAMPS) and second network (PAAm), respectively. For both networks, N, N′-methylenebisacrylamide (MBAA; Aladdin) and 2-oxoglutaric acid (OA; Aladdin) were used as the crosslinker and radical initiator, respectively. For the first network, the feed concentrations of the monomer (AMPS), crosslinker (MBAA), and radical initiator (OA) were 1 M, 20 mM, and 2 mM, respectively. For the second network, the feed concentrations of the monomer (AAm), crosslinker (MBAA), and radical initiator (OA) were 2 M, 0.4 mM, and 2 mM, respectively. The precursor solution of the first network was poured into a glass mold and cured under UV light (80 W, 365 nm). The synthesized first-network hydrogel PAMPS was then immersed in a large amount of the precursor solution of the second network for at least one day to be fully swollen. Afterwards, it was placed between a pair of glass plates and cured again under UV light. The irradiation time for the polymerization of the first and second networks was 10 h. For the PAMPS and PAAm hydrogels, the same feed concentration and irradiation time as those of the first and second networks in the DN gel were used for synthesis.

2.2. Mechanical tests for the DN gel and its components

2.2.1. Uniaxial tensile test

To characterize the stress–stretch relationship and dissipated energy density of DN gels under uniaxial tension, we carried out two types of uniaxial tensile tests for the DN gels: monotonic loading and cyclic loading tests. Both tests were conducted on dumbbell-shaped samples by a tensile test machine (SHIMADZU AGS-X; 1000 N load cell). The sample had an initial gauge length of 20 mm, and a width and thickness of 4 mm and 1.5 mm, respectively. To investigate the effects of the loading speed on the deformation behavior, we conducted monotonic tensile tests at different loading velocities from 50 mm/min to 200 mm/min. The stress–stretch relationship of DN gels was found to be rate-independent in this range. Therefore, a loading velocity of 100 mm/min was used.

We obtained the stress–stretch relationship by conducting a monotonic loading test, as shown in Fig. 1a. It is generally considered that the whole loading curve of DN gels can be divided into three regions: prenecking, necking, and hardening (Nakajima et al., 2013). In the prenecking region, the stress increases monotonically with the stretch until it reaches the necking point, at which the necking begins. In the necking region, the stress remains constant as the stretch increases, and the DN gel exhibits a yielding behavior. As the stretch further increases, the DN gel exhibits a hardening behavior and the stress once again increases.

During cyclic loading, the DN gel performs large hysteresis loops, as shown in Fig. 1b. The dissipated energy density of DN gels is dependent on the maximum historical stretch, and can be measured by the area of the hysteresis loop at the corresponding stretch. The value of dissipated energy density can be used to calculate the dissipated fracture energy in the pre-yield and yield fields.

2.2.2. 180-degree peeling test

To better understand the fracture toughness of the DN gel, the fracture properties of its component single-network hydrogels (PAMPS and PAAm hydrogels) were clarified. Because the PAMPS hydrogel is too fragile to be subjected to other types of fracture tests, such as tearing and pure shear tests, we carried out the 180-degree peeling test to compare the toughness of the DN gel and its component single-network hydrogels.

In the 180-degree peeling test (Fig. 2a), a hydrogel sample with a length of 100 mm and width of 10 mm was first coated with an

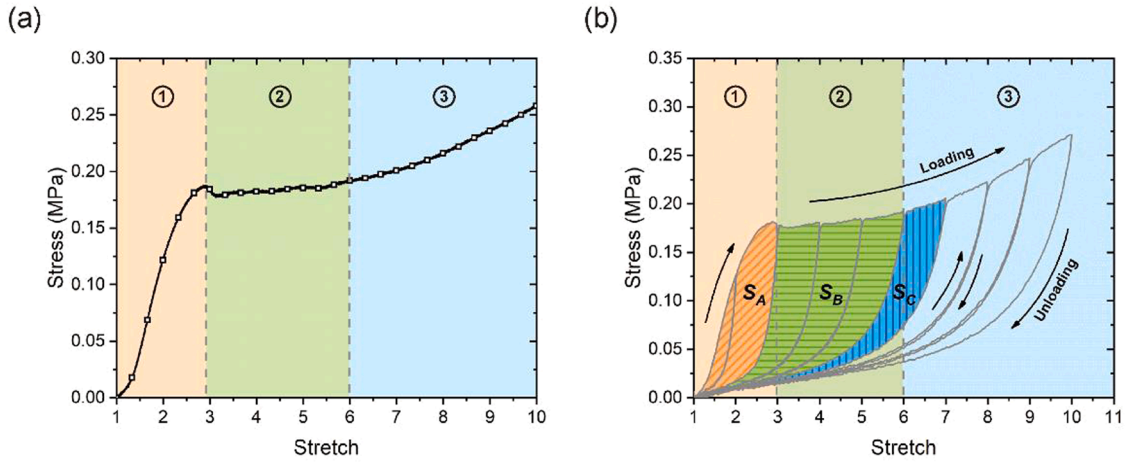

Fig. 1. Stress-stretch curves under uniaxial tensile tests of DN gels. (a) Monotonic loading curve of a DN gel. (b) Cyclic loading curve of a DN gel. The curves can be divided into three regions: ① prenecking, ② necking, and ③ hardening region.

adhesive primer (DGGULI) and then glued to a soft but inextensible backing (Scotch tape; 3M) on both sides by cyanoacrylate (Loctite; Hendel). The thicknesses of the DN gel and two single-network hydrogels used in this test were 3 mm and 2 mm, respectively. The hydrogel sample was precut using a razor blade. To investigate the effect of the primer on the mechanical properties of the DN gel, we performed the uniaxial tensile test on the DN gel with and without the primer. We found that the primer had no effect on the mechanical properties of DN gels. The peeling toughness was calculated by the following equation (Gent, 1974; Gent and Hamed, 1977)

$$\Gamma = \frac{2F_c}{w} \tag{2}$$

where w is the width of the specimen and F_c is the average peeling force when it reaches a plateau. The toughness of the three types of hydrogels measured by the peeling tests are $10 \pm 1\ \mathrm{J/m^2}$ (PAMPS), $126 \pm 1\ \mathrm{J/m^2}$ (PAAm), and $2616 \pm 220\ \mathrm{J/m^2}$ (DN gel), as shown in Fig. 2b.

2.2.3. Tearing test

Tearing test is a common method for measuring the toughness of DN gels. A trouser-shaped sample is usually adopted, and the toughness is calculated by (Long and Hui, 2016; Rivlin, 1953)

$$\Gamma = \frac{2F_c\lambda_c}{t} - 2wW_c \tag{3}$$

where F_c is the average plateau force, λ_c is the average stretch of the leg, W_c is the average elastic energy density of the leg when the crack propagation reaches a steady state, t is the thickness of the tearing specimen, and w is the width of one leg. To simplify the calculation of the toughness, we used a trouser-shaped specimen with backings on the legs (Fig. 3a). The backing has a relatively low bending stiffness and high tensile stiffness compared with DN gels. In this case, the elongation of the leg is constrained, and λ_c and W_c can be approximated as one and zero, respectively. Therefore, the toughness for the tearing test with backings on the legs is simplified from Eq. (3) as

$$\Gamma = \frac{2F_c}{t} \tag{4}$$

A typical force-displacement curve of the DN gel during our tearing test is shown in Fig. 3b.

To study the effect of the dissipation zone on the fracture toughness of DN gels, we introduce a new parameter in the tearing test, the free width b, which represents the distance between the two backings of the trouser-shaped sample (Fig 3a). We chose the tearing test because the value of b is directly related to the size of the damage zone, and b can be easily controlled by adjusting the distance between two backings. Here, we measured the toughness of DN gels with different b values ranging from 0 mm to 10 mm. When $b = 0$ mm, the deformation of crack tip field is completely constrained by the backing, it is considered that there is no dissipation zone during the fracture process, $\Gamma_d = 0$. Therefore, the measured fracture energy is the intrinsic fracture energy, i.e., $\Gamma = \Gamma_0$. It is worth mentioning that although we changed the distance between the two backings, the elongations of the legs of the sample were still constrained, and Eq. (4) can be applied to obtain the tearing toughness of DN gels. It should also be noted that the tearing method used for $b = 0$ is slightly different from the method used for $b \neq 0$. When $b \neq 0$, the F_c in Eq. (4) is the average plateau force during loading. However, when $b = 0$, the trouser-shaped specimen is torn along with the backing. Thus, the loading force during tearing is the total force required to simultaneously tear the DN gel and backing. In this case, the F_c in Eq. (4) should be modified as

$$F_c = F_{total} - F_{backing} \tag{5}$$

where F_{total} is the plateau force to tear both the DN gel and backing, and $F_{backing}$ is the plateau force to tear just the backing. The experimental images of the tearing tests with different free widths b are shown in Fig. 4. The entire tearing process is provided in Video

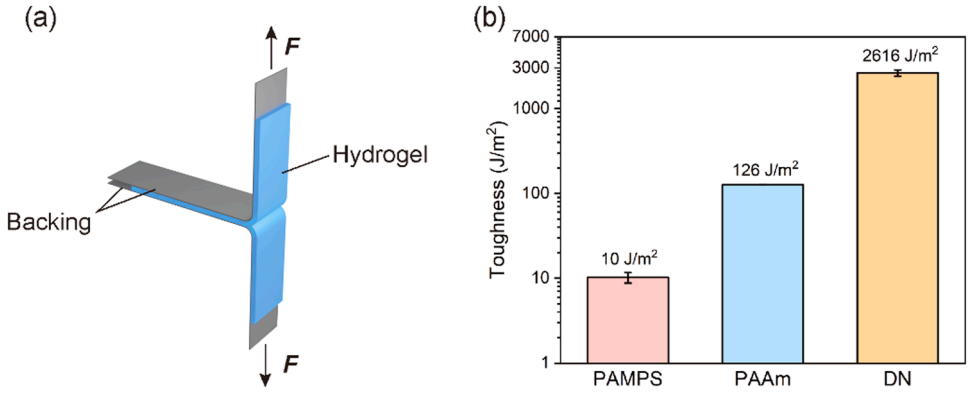

Fig. 2. 180-degree peeling test. (a) Experimental setup. (b) The toughness of PAMPS, PAAm, and DN gels measured by the 180-degree peeling test.

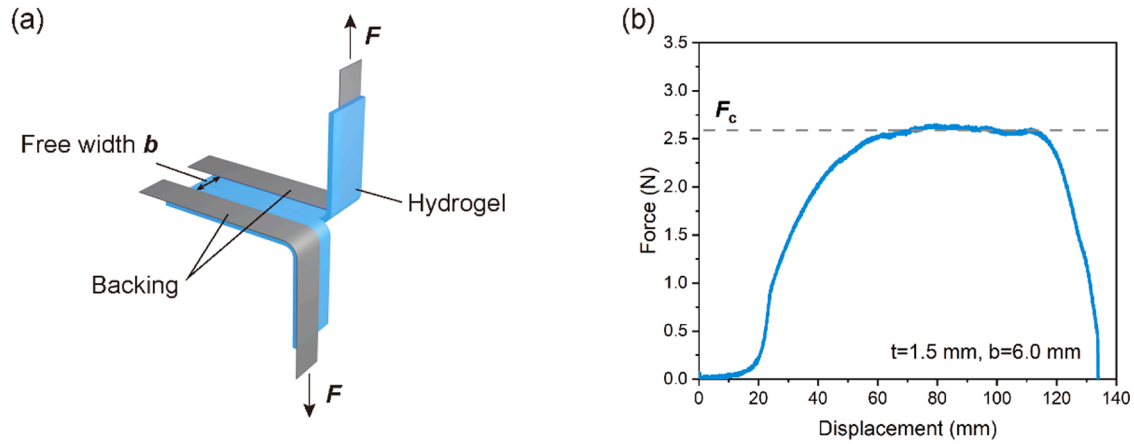

Fig. 3. Tearing test. (a) Experimental setup. (b) Force−displacement curve of a trouser-shaped DN gel specimen during the tearing test.

S1.

In the tearing test, the following parameters of the specimen were adopted. For $b = 0$, the length and width of the specimen are 50 mm and 30 mm, respectively, with an initial cut of ~ 10 mm by a pair of scissors. For $b \neq 0$, the length and width of the specimen are 70 mm and 30 mm, respectively, with an initial cut of 15 mm. The thickness of all tearing specimens is 1.5 mm. It should be noted that the initial crack length is considered to have no influence on the average plateau force F_c according to our experiments.

3. Fracture toughness of DN gels

3.1. Effect of free width b on the toughness of tearing

From our tearing test results, we obtained the relationship between the apparent toughness Γ and free width b, as shown in Fig. 5. It can be seen that as b increases from 0 mm to 10 mm, the apparent toughness Γ first increases and then plateaus. The plateau value of the apparent toughness Γ is denoted as the plateau toughness Γ_p. From Eq. (1), the apparent toughness Γ can be divided into the intrinsic fracture energy Γ_0 and dissipated fracture energy Γ_d. The dissipated fracture energy Γ_d is contributed by the energy dissipation in the crack-tip field when the crack propagates along a unit area. When b is set as 0, the deformation of the crack-tip field is constrained by the backing and cannot dissipate energy; hence, Γ_d can be eliminated and $\Gamma = \Gamma_0$.

We propose an exponential function to describe the quantitative relationship between Γ and b based on Fig. 5

$$\Gamma = -a_1 * e^{-a_2 b} + a_3 \tag{6}$$

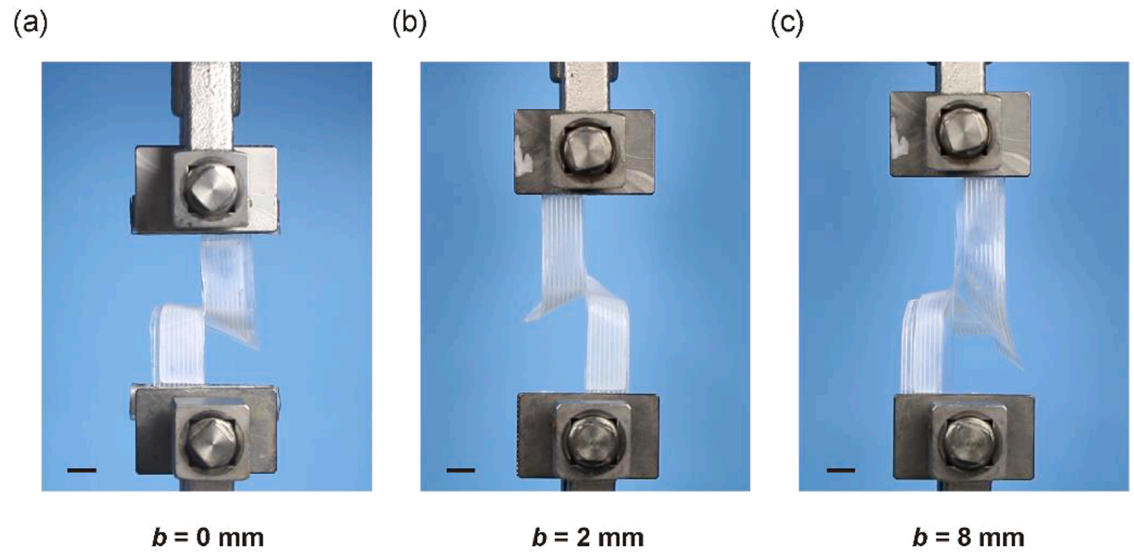

Fig. 4. Experimental images of tearing tests with different free widths b. (a) $b = 0$ mm. (b) $b = 2$ mm. (c) $b = 8$ mm. The scale bars represent 1 cm.

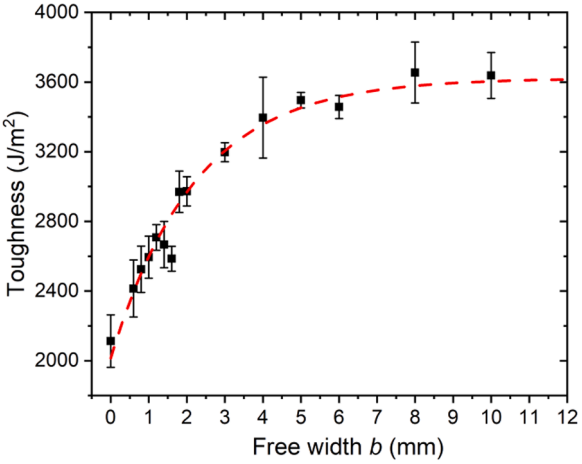

Fig. 5. Relationship between the apparent toughness Γ and free width b.

where a_1, a_2, and a_3 are the fitting parameters (a_1, a_2, and a_3 have positive values). Through Eq. (6), we can obtain the physical meaning of these parameters by considering two extreme conditions. When $b \to +\infty$, $\Gamma = a_3 = \Gamma_p$, Thus, a_3 represents the plateau toughness Γ_p. When $b \to 0$, $\Gamma = a_3 - a_1 = \Gamma_0$. Recall that a_3 is the plateau toughness Γ_p, then a_1 should be the dissipated fracture energy Γ_d when $\Gamma = \Gamma_p$. When $b = 0$, the derivative of Eq. (6) is $a_1 a_2$, which means that the initial slope of Eq. (6) increases with a_2 (a_1 is set as a constant). With a higher value of a_2 (a_1 and a_3 are set as constants), the apparent toughness Γ will reach the plateau toughness Γ_p with a smaller value of b.

Based on this relationship between Γ and b, a transition value of b exists, above which Γ tends to be a constant. This transition value of b is defined as a feature size of the dissipation zone of DN gels, and is denoted by l_d. Mathematically, l_d is determined as the value of b when the apparent toughness reaches $0.99 * \Gamma_p$. Therefore, we have

$$-a_1 * e^{-a_2 l_d} + a_3 = 0.99 a_3 \tag{7}$$

$$l_d = \frac{lna_1 - ln0.01a_3}{a_2} \tag{8}$$

By fitting Eq. (6) with the experimental results in Fig. 5, a_1, a_2, and a_3 are obtained as 1607, 0.45, and 3622, respectively. Thus, Eq. (6) becomes

$$\Gamma = -1607 * e^{-0.45b} + 3622 \tag{9}$$

By studying Eq. (9), the plateau toughness Γ_p is 3622 J /m^2 and the intrinsic fracture energy Γ_0 is 2015 J /m^2 for the DN gels used in

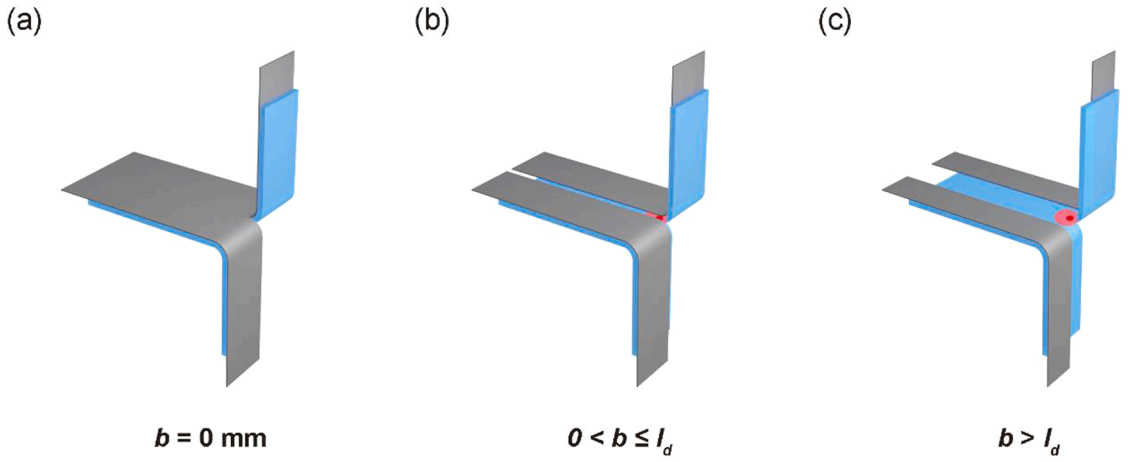

Fig. 6. The dissipation zone in the crack tip field of DN gels with different values of b. (a) When b is zero, there is no dissipation zone around the crack tip. (b) When b is greater than zero and smaller than the feature size of the dissipation zone l_d, the dissipation zone is restricted by b. (c) When b is larger than l_d, the dissipation zone does not change with b.

this study. When $\Gamma = \Gamma_p$, the dissipated fracture energy Γ_d is 1607 J /m^2. By substituting the values of a_1, a_2, and a_3 into Eq. (8), the feature size of the dissipation zone l_d is calculated as 8.5 mm. Interestingly, the intrinsic fracture energy Γ_0 (2015 J /m^2) measured in this study is of the same order of magnitude as the dissipated fracture energy Γ_d (1607 J /m^2), and much larger than the fracture energy of the pure second-network hydrogel PAAm $\Gamma_{2nd-network}$ (126 J /m^2 in Fig. 2b). This indicates that the contribution of Γ_0 to the total fracture energy cannot be neglected.

The relationship between the apparent fracture energy Γ and free width b confirms the existence of a large dissipation zone in the DN gels. The mechanism behind the experimental results in Fig. 5 can be explained as follows. When b is zero, the deformation of the crack-tip field is restricted, and it has no dissipation zone (Fig. 6a). The measured value of Γ is the intrinsic fracture energy Γ_0. When b is greater than zero and smaller than the feature size of the dissipation zone l_d ($0 < b \leq l_d$), the actual size of the dissipation zone is determined by b (Fig. 6b). As a result, the value of Γ is smaller than Γ_p with less dissipated energy in the crack-tip field, and increases as b increases. When b is larger than the feature size of the dissipation zone l_d, the size of the dissipation zone during crack propagation is l_d and does not change with an increase in b (Fig. 6c); thus, the apparent toughness reaches the plateau Γ_p.

According to the work of Bai et al. (2019), the tearing toughness of tough gels, which is a type of DN hydrogel, may depend on the thickness of the specimen. To investigate the influence of thickness on toughness, we repeated the peeling test with a specimen thickness of 3 mm and b of 0 mm. The intrinsic fracture energy of 2329 $\pm$ 32 J /m^2 was obtained, which is close to the intrinsic fracture energy of 2113 $\pm$ 151 J /m^2 obtained in the previous test with a specimen thickness of 1.5 mm. These results show that the toughness of the DN gel was not affected by the increase in thickness from 1.5 mm to 3 mm. Thus, in this study, we did not consider the influence of thickness on the tearing test results.

3.2. Decomposition of fracture energy and feature size of the damage zone

To elucidate the relationship between the deformation states of the crack-tip field and fracture energy Γ, the crack-tip field is divided into four regions according to their deformation states (Fig. 7): elastic, pre-yield, yield, and intrinsic fields. The pre-yield, yield, and intrinsic fields constitute the damage zone. Polymer chain scission in the first or second network occurs in these fields and contributes to the toughness of the DN gels.

In the elastic field, the deformation of DN gels is relatively small and without the occurrence of damage. The DN gels in this field remain elastic and do not contribute dissipated energy to the toughness Γ. The pre-yield and yield fields are collectively referred to as the dissipation field. The stress in the dissipation field is greater than that in the elastic field owing to the stress concentration around the crack tip. Damage accumulation occurs in the dissipation field, and the dissipated energy in this field contributes to the value of Γ_d. In the dissipation field, only the polymer chains in the first network rupture to dissipate energy, whereas the polymer chains in the second network do not break. In the intrinsic field, the polymer chains in both networks rupture to allow crack propagation, contributing to the intrinsic fracture energy Γ_0.

Despite the complexity of the stress state of the crack tip in the tearing test, the uniaxial tensile result was adopted as an approximation to describe the crack-tip deformation state (Matsuda et al., 2020; Matsuda et al., 2021). The deformation states of DN gels in the pre-yield and yield fields were assumed to correspond to the deformation states (i.e., ① prenecking region and ② necking region) in the uniaxial tensile test (Fig. 1).

During crack propagation, the dissipated energy density is maximized at the crack surface owing to the stress concentration and decreases along the z-direction (Fig. 8a) (Matsuda et al., 2021). The distribution of the dissipated energy density indicates the degree of internal damage in the DN gels. By integrating the dissipated energy density U_{diss} in the z-direction, we obtain the value of Γ_d (Long and Hui, 2016)

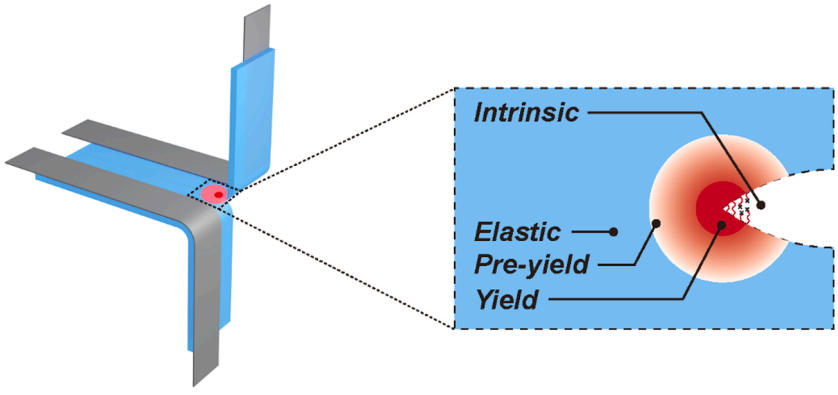

Fig. 7. Deformation fields in the crack tip, i.e. elastic, pre-yield, yield, and intrinsic field.

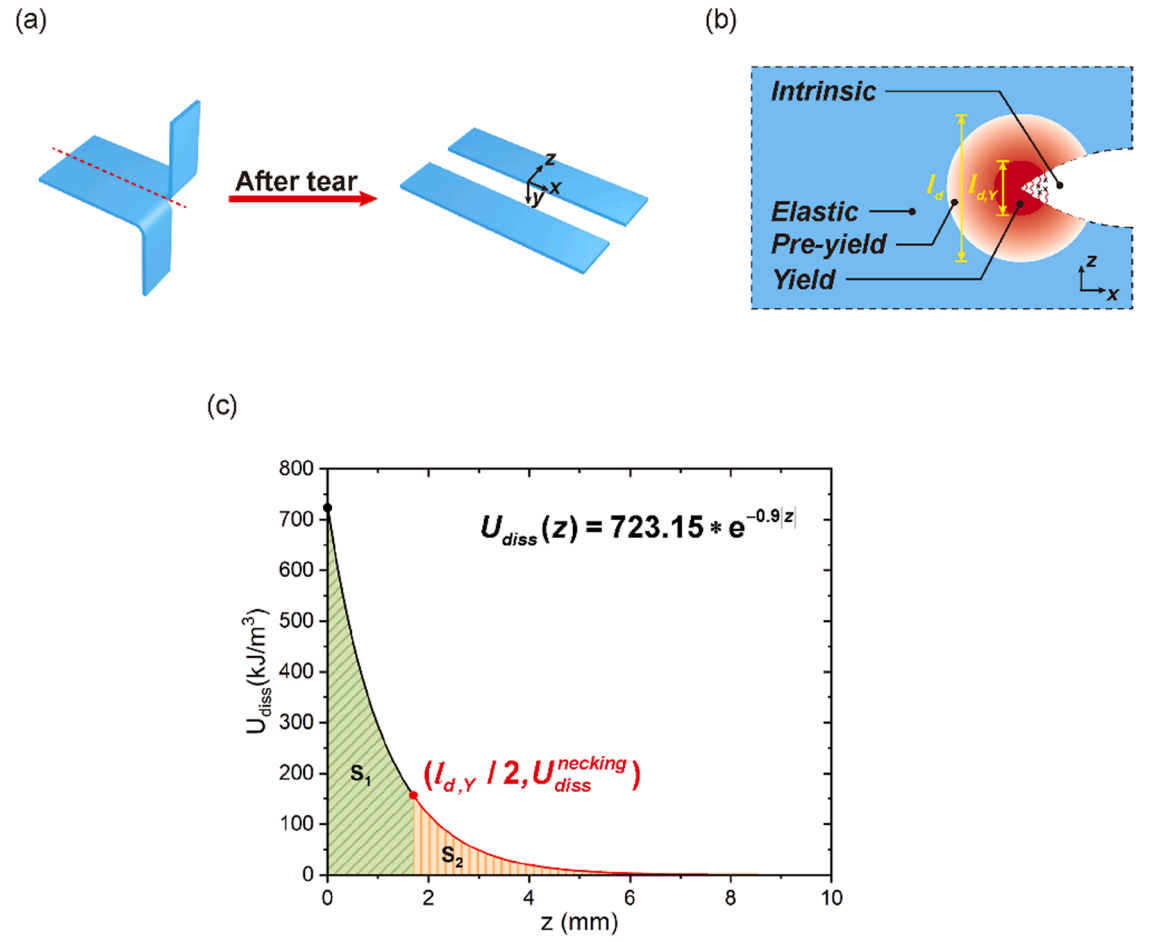

Fig. 8. The coordinates of the tearing specimen and the dissipated energy density U_{diss} in the crack-tip field. (a) Schematic illustration of a fractured tearing specimen and the (x, y, z) coordinates. (b) Feature sizes of the dissipation field and yield field. (c) U_{diss} at different coordinates along the axial of z ($z \geq 0$).

$$\Gamma_d(b) = 2\int_0^{\frac{b}{2}} U_{diss}(z)dz \tag{10}$$

From Eq. (1), Γ is a component of Γ_d and Γ_0. Therefore, the apparent toughness Γ can be calculated as

$$\Gamma(b) = 2\int_0^{\frac{b}{2}} U_{diss}(z)dz + \Gamma_0 \tag{11}$$

By substituting Eq. (9) into Eq. (11) and taking the derivative of Eq. (11), we obtain

$$\frac{d\Gamma(b)}{db} = U_{diss}(b/2) = 723.15 * e^{-0.45b} \tag{12}$$

We assume that the function of $U_{diss}(z)$ is independent of the value of b, and replace b with $2|z|$. Thus, we obtain the dissipated energy density at different coordinates along the z-axis

$$U_{diss}(z) = 723.15 * e^{-0.9|z|} \tag{13}$$

According to Eq. (13), the dissipated energy density U_{diss} at different coordinates along the z-axis ($z \geq 0$) is plotted in Fig. 8c. As mentioned above, the dissipated energy in the pre-yield and yield fields contribute to Γ_d

$$\Gamma_d = \Gamma_{d,P} + \Gamma_{d,Y} \tag{14}$$

where $\Gamma_{d,P}$ and $\Gamma_{d,Y}$ is the dissipated energy in the pre-yield and yield fields, respectively, when the crack propagates along a unit area.

Obtaining the function of $U_{diss}(z)$ in Eq. (13), the dissipated fracture energy in the pre-yield field $\Gamma_{d,P}$ and yield field $\Gamma_{d,Y}$ can be calculated by integrating $U_{diss}(z)$ in the z-direction as follows

$$\Gamma_{d,P} = 2\int_{\frac{l_{d,Y}}{2}}^{\frac{l_d}{2}} U_{diss}(z)dz \tag{15}$$

$$\Gamma_{d,Y} = 2\int_{0}^{\frac{l_{d,Y}}{2}} U_{diss}(z)dz \tag{16}$$

where l_d and $l_{d,Y}$ is the feature size of the dissipation and yield fields, respectively (Fig. 8b). The feature size of the pre-yield field is denoted as $l_{d,P}$: $l_{d,P} = l_d - l_{d,Y}$. The values of $\Gamma_{d,Y}$ and $\Gamma_{d,P}$ correspond to $2S_1$ and $2S_2$, as shown in Fig. 8c.

From Fig. 8c, it can be seen that in the dissipation zone, the value of U_{diss} decreases with the increase in $|z|$. At the edge of the dissipation zone (Fig. 8b), U_{diss} decreases to zero ($U_{diss}\left(\frac{l_d}{2}\right) = 0$). According to Matsuda et al. (2021), the maximum dissipated energy density in the pre-yield field occurs at the edge between the pre-yield and yield fields, which is $U_{diss}\left(\frac{l_{d,Y}}{2}\right)$. The value of $U_{diss}\left(\frac{l_{d,Y}}{2}\right)$ is the dissipated energy density at the necking point determined by the uniaxial cyclic tensile test, and corresponds to the area S_A in Fig. 1b. Substituting $\frac{l_{d,Y}}{2}$ as z into Eq. (13), we obtain

$$U_{diss}\left(\frac{l_{d,Y}}{2}\right) = 723.15 * e^{-0.9\frac{l_{d,Y}}{2}} = S_A \tag{17}$$

According to Fig. 1b, the value of S_A is 155.22 kJ $/m^3$. Thus, the feature size of the yield field $l_{d,Y}$ is 3.4 mm. It is worth noting that in the yield field, the maximum U_{diss} (723.15 kJ $/m^3$) at $z = 0$ (Fig. 7c) is very close to the area of $S_A + S_B + S_C$ (730.63 kJ $/m^3$), which is the total dissipated energy density when the DN gels complete the necking stage in the uniaxial tensile test (Fig. 1b). The obtained U_{diss} in the crack-tip field corresponds to the dissipated energy density of the DN gels in the uniaxial tensile test. The relationship between the total dissipated energy density and maximum deformation state of the DN gels is monotonic (Fig. 1b). The above findings validate our assumption that the deformation states of DN gels in the pre-yield and yield fields correspond to the deformation states in the uniaxial tensile test.

All the feature sizes of the dissipation zone are now obtained. The feature size of the dissipation field l_d is 8.5 mm, the feature size of the yield field $l_{d,Y}$ is 3.4 mm, and the feature size of the pre-yield field is 5.1 mm ($l_{d,P} = l_d - l_{d,Y}$). Substituting the values of $l_{d,Y}$ and l_d into Eqs. (15) and (16), the dissipated fracture energy in the pre-yield field $\Gamma_{d,P}$ is estimated as 347 J $/m^2$, while that in the yield field $\Gamma_{d,Y}$ is estimated as 1260 J $/m^2$.

Up to now, we have successfully decomposed Γ_d and l_d into their components. The decomposition process of Γ_d and l_d has an explicit physical meaning and leads to a deeper understanding of how the deformation of the crack-tip material influences the toughness value. Based on our finding that most of the energy dissipation occurs in the yield field ($\Gamma_{d,Y} > \Gamma_{d,P}$), DN gels that exhibit an apparent necking phenomenon may have a higher toughness value, which can guide the design of DN gels for practical use. In addition, because the large dissipated fracture energy Γ_d of DN gels is attributed to a large dissipation zone, if their deformation is excessively restricted, then the advantage of DN gels in resisting crack propagation cannot be properly nor fully exploited. Therefore, we recommend that sufficient free space be retained when using DN gels, at least in the size of $l_{d,Y}$.

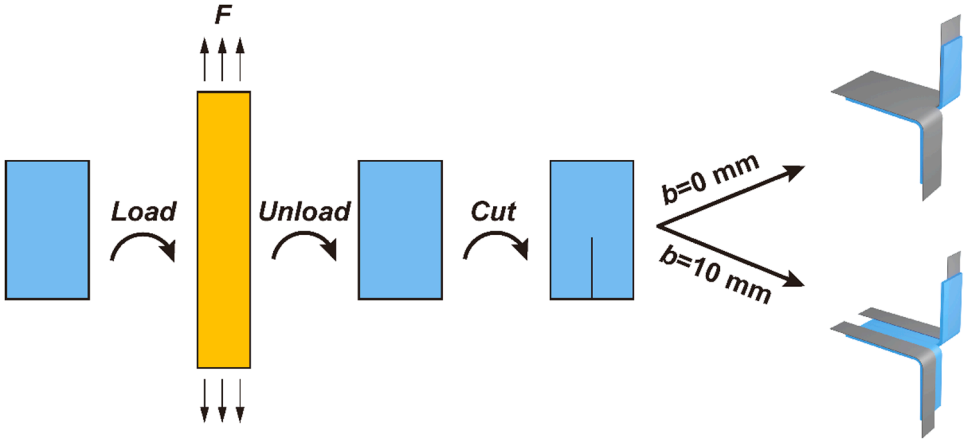

Fig. 9. DN gel is prestretched before the tearing test.

3.3. Effect of prestretch on the toughness of tearing

For DN gels, damage accumulates during deformation, as shown in Fig. 1b. The degree of damage of DN gels is determined by their maximum historical deformation. To determine the influence of the historical deformation on the fracture energy of DN gels, we conducted the following experiments.

We first loaded the specimen in one direction to a relatively large stretch of eight, at which the DN gel has reached the hardening region, and then unloaded the specimen. We defined the DN gel specimen that was preloaded before the tearing test as the prestretched DN gel. Similarly, the DN gel specimen with no historical deformation before the tearing test was denoted as the as-prepared DN gel. Then, we performed tearing tests on the prestretched specimen with $b = 0$ mm and 10 mm, and obtained the corresponding toughness. The experimental process is shown in Fig. 9 with a specimen size of 50 mm long, 30 mm wide, and 1.5 mm thick. The crack propagation direction was set to be the same as the preloading direction to avoid the influence of damage anisotropy. The residual deformation due to loading was found to be negligible in our experiments.

By performing tearing tests on the prestretched and as-prepared samples with free widths $b = 0$ mm and 10 mm, we obtained the intrinsic fracture energy Γ_0 and plateau toughness Γ_p for these two types of specimens (Fig. 10). From Fig 10, it can be seen that the Γ_0 values for prestretched and as-prepared DN gels are $1321 \pm 123\,\mathrm{J/m^2}$ and $2113 \pm 151\,\mathrm{J/m^2}$, while the Γ_p values are $1311 \pm 105\,\mathrm{J/m^2}$ and $3638 \pm 132\,\mathrm{J/m^2}$, respectively. Interestingly, it can be seen that for prestretched DN gels, the Γ_0 and Γ_p values are nearly the same, and both are smaller compared with those of the as-prepared DN gels.

It can be inferred that the apparent toughness Γ is related to the historical deformation because the damage to the PAMPS chains is irreversible. After prestretching, there will be fewer effective PAMPS chains in the DN gel. During crack propagation, the remaining undamaged PAMPS chains will contribute less to the dissipated energy and reduce Γ_d. Therefore, we can conclude that after prestretching, the DN gel has a smaller Γ_p value compared with that of the as-prepared DN gel. When the prestretch is sufficiently large, there are few effective PAMPS chains remaining in the DN gel to dissipate energy, and the dissipated fracture energy Γ_d is close to zero. Thus, the Γ_0 value will be close to Γ_p after a large prestretch.

With regard to the intrinsic fracture energy Γ_0 of DN gels, Γ_0 is usually considered as the material property, which means that it is a constant regardless of the historical deformation. Besides, it is often assumed that the Γ_0 of DN gels is of the same order of magnitude as the toughness of its PAAm hydrogel component (Brown, 2007; Tanaka, 2007). Although these opinions are widely accepted, they may not be true according to the results of our experimental study. In our experiment, the Γ_0 of as-prepared and prestretched DN gels were measured as $2113 \pm 151\,\mathrm{J/m^2}$ and $1321 \pm 123\,\mathrm{J/m^2}$, respectively. This large difference demonstrates that the Γ_0 of DN gels is dependent on the historical deformation. In addition, our experimental results show that the two Γ_0 values are significantly larger than the PAAm hydrogel toughness Γ_{PAAm} of $126 \pm 1\,\mathrm{J/m^2}$ (Fig. 2b).

Unfortunately, to the best of our knowledge, there is no model that can properly explain why the Γ_0 of DN gels is much higher than the toughness of its component hydrogels, and why it is dependent on the historical deformation. In the next section, we propose a model to predict the Γ_0 of DN gels. A physical interpretation is given on the origin of the Γ_0, and the reason why it decreases after prestretching.

4. Modeling of the intrinsic fracture energy

The intrinsic fracture energy of polymer networks can be described by the Lake–Thomas model (Lake et al., 1967), in which the intrinsic fracture energy is calculated as the energy required to fracture a single layer of polymer chains in a perfect network without defects. For single-network hydrogels, a modified form of the Lake–Thomas model is (Tang et al., 2017)

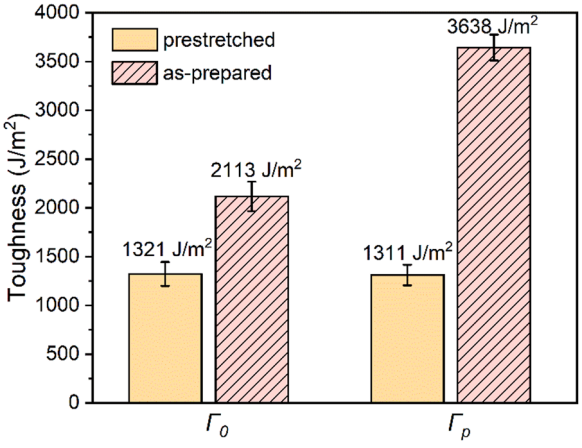

Fig. 10. Comparison of intrinsic fracture energy Γ_0 and plateau toughness Γ_p between prestretched DN gels and as-prepared DN gels.

$$\Gamma_0 = \phi^{\frac{2}{3}}\sqrt{n}aUl \tag{18}$$

where ϕ is the volume fraction of the polymer chains in the hydrogel, n is the number of monomers between two crosslinks, a is the number of single bonds per unit volume of the dry polymer, U is the energy required to break a chemical bond, and l is the length of the monomer.

In the Lake–Thomas model, the polymer network is abstracted by the affine network model. The affine network model assumes that the ends of the polymer chains are fixed to an elastic background, which means that the scission of a single polymer chain will not affect the surrounding polymer chains. Thus, the Lake–Thomas model only considers the energy required to break a single layer of polymer chains and neglects the contribution of surrounding polymer chains, which may underestimate the intrinsic fracture energy of real polymers.

Lin et al. modified the traditional Lake–Thomas model based on the phantom network model (Lin and Zhao, 2020). In the phantom network model, most of the ends of polymer chains are not fixed to an elastic background and can fluctuate in the polymer network. Therefore, when one polymer chain ruptures, the surrounding polymer chains adapt their deformation states to lower energy states and release the elastic energy that was previously stored in the surrounding polymer chains. According to Lin et al., for an ideal polymer network without defects, the intrinsic fracture energy is $\frac{f}{f-2}$ times the value predicted by the traditional Lake–Thomas model (Lin and Zhao, 2020), where f is the degree of crosslinking, which is the number of polymer chains at each crosslinking point. Based on the work of Lin et al., for an ideal polymer network, the intrinsic fracture energy of a single-network hydrogel is

$$\Gamma_0^{ph} = \frac{f}{f-2}\phi^{\frac{2}{3}}\sqrt{n}aUl \tag{19}$$

For DN gels, there are two penetrating polymer networks in the hydrogel: the PAMPS network, which is rigid and brittle; and the PAAm network, which is soft and stretchable. The PAAm network has much longer polymer chains compared with the PAMPS network. Thus, a large number of PAMPS polymer chains will rupture prior to crack propagation, and it is the scission of PAAm polymer chains that will finally allow the crack propagation in DN gels.

According to the modified Lake–Thomas model in Eq. (19), the energy required to break a single layer of PAAm chains in DN gels is

$$\Gamma_0^{PAAm} = \frac{f}{f-2}\left(\phi_{PAAm}^{DN}\phi_{AAm}^{PAAm}\right)^{\frac{2}{3}}\sqrt{n_{AAm}}a_{AAm}Ul_{AAm} \tag{20}$$

where $\phi_{PAAm}^{DN}\phi_{AAm}^{PAAm}$ is the volume fraction of the PAAm polymer chains in the DN gel, ϕ_{PAAm}^{DN} is the volume fraction of PAAm hydrogel in the DN gel, ϕ_{AAm}^{PAAm} is the volume fraction of the polymer chains in the pure PAAm hydrogel, n_{AAm} is the number of monomers between two crosslinks in PAAm chains, a_{AAm} is the number of single bonds per unit volume of the dry PAAm polymer, U is the energy required to break a C-C bond, and l_{AAm} is the length of the AAm monomer.

However, in the DN gel, the two interpenetrating networks are closely entangled, and it is impossible to break a single layer of PAAm chains without affecting the PAMPS chains. Thus, we believe that both PAAm and PAMPS networks contribute to the intrinsic fracture energy of DN gels expressed as

$$\Gamma_0^{DN} = \Gamma_0^{PAAm} + \Gamma_0^{PAMPS} \tag{21}$$

where Γ_0^{DN} is the intrinsic fracture energy of the DN gel, and Γ_0^{PAAm} and Γ_0^{PAMPS} are the contributions of the PAAm and PAMPS networks to Γ_0^{DN}, respectively.

According to the phantom network theory (Lin and Zhao, 2020), for an ideal polymer network, the chains within layers of $|i| \leq 5$ (i represents the sequence of polymer chain layers to the ruptured layer) around the ruptured chain layer will contract to release the stored elastic energy (see Supporting Note I in the Supplementary Materials). Therefore, within the range of $|i| \leq 5$ in the PAAm network, the PAMPS chains in the field will also rupture to release energy. It is worth noting that since the PAAm chains are much longer than the PAMPS chains, we estimate the area within which the PAMPS chains are affected by taking into account of the influence of the rupture of PAAm chains. The rupture of one layer of PAMPS chains will also affect other PAMPS chains. However, this area is much smaller than the area affected by the rupture of PAAm chains. The energy required to break all the PAMPS chains in the field, because of the rupture of the PAAm network, is calculated as

$$\Gamma_0^{PAMPS} = \phi_{PAMPS}^{DN}\phi_{AMPS}^{PAMPS}a_{AMPS}\left(2|i|_{max}+1\right)\left(\sqrt{n_{AAm}}\,l_{AAm}\right)\left(\phi_{PAAm}^{DN}\phi_{AAm}^{PAAm}\right)^{-\frac{1}{3}}U \tag{22}$$

where $\phi_{PAMPS}^{DN}\phi_{AMPS}^{PAMPS}$ is the volume fraction of the PAMPS polymer chains in the DN gel, $\phi_{PAMPS}^{DN}\phi_{AMPS}^{PAMPS}a_{AMPS}$ is the number of AMPS monomer in a unit volume of DN gel, $(\sqrt{n_{AAm}}\,l_{AAm})(\phi_{PAAm}^{DN}\phi_{AAm}^{PAAm})^{-\frac{1}{3}}$ is the thickness of one layer of PAAm network in DN gel, and $(2|i|_{max}+1)$ is the number of layers of PAAm network chains affected by the rupture of one layer of PAAm chains. Therefore, $(2|i|_{max}+1)(\sqrt{n_{AAm}}\,l_{AAm})(\phi_{PAAm}^{DN}\phi_{AAm}^{PAAm})^{-\frac{1}{3}}$ is the thickness of the affected field within which all the PAMPS chains rupture to release energy. For an ideal polymer network, the $|i|_{max}$ is 5.

In Eq. (20), we obtained the energy required to break a single layer of PAAm chains in DN gels without considering the influence of the PAMPS network. Previous studies showed that the ruptured PAMPS chains will aggregate to form rigid fragments that act as crosslinking points for the PAAm chains (Gong, 2010; Nakajima et al., 2013). Thus, for the PAAm chains that are about to rupture in

DN gels, the number of monomers between two crosslinks will increase to $n_{AAm}|i|_{max}$ because of the large crosslinking points formed by the PAMPS chains. Consequently, Eq. (20) can be modified as

$$\Gamma_0^{PAAm} = \frac{f}{f-2}\left(\phi_{PAAm}^{DN}\phi_{AAm}^{PAAm}\right)^{\frac{2}{3}}\sqrt{n_{AAm}|i|_{max}}a_{AAm}Ul_{AAm} \tag{23}$$

Considering the interaction between the two interpenetrating networks, Γ_0^{DN} is the summation of Γ_0^{PAAm} in Eq. (23) and Γ_0^{PAMPS} in Eq. (22).

The parameters mentioned above are calculated in Supporting Note II in the Supplementary Materials. By substituting the values of these parameters into Eqs. (22) and (23), for an ideal network without defects, Γ_0^{PAMPS} and Γ_0^{AAm} were calculated as 7.71 J /m^2 and 164.04 J /m^2, respectively. The intrinsic fracture energy of the DN gel is 171.75 J /m^2, which is much lower than the measured $\Gamma_0 \sim$ 2000 J /m^2 for the as-prepared DN gel in our experiment.

Note that a real polymer network has many types of imperfections, such as loops, dangling chains, clusters, cavities, and entanglements; and exhibits a complex hierarchical structure Li et al., 2021; Seiffert, 2017). Thus, for a real polymer network, the rupture of one layer of chains may influence hundreds of surrounding layers; hence, the $|i|_{max}$ may be greater than 5 for an ideal network. According to our experiments, the intrinsic fracture energy of as-prepared DN gels is 2113 $\pm$ 151 J /m^2. Substituting the measured Γ_0 into Eq. (21), and combining Eqs. (21)–((23), $|i|_{max}$ was estimated as 865. Then, the contribution of single-network hydrogels to the fracture energy of DN gels was calculated as $\Gamma_0^{PAMPS} = 607$ J /m^2 and $\Gamma_0^{PAAm} = 1507$ J /m^2.

For fully prestretched DN gels, the Γ_0 value was measured as 1321 $\pm$ 123 J /m^2, which is close to the Γ_0^{PAAm} value obtained from our model. This is because the PAMPS chains already ruptured during the preloading process, and Γ_0^{PAMPS} did not contribute to Γ_0. Even after prestretching, the Γ_0 of the DN gels remained much larger than the fracture energy of pure PAAm hydrogels. According to our model, the reason could be as follows. Although the PAMPS chains had already ruptured during the preloading process, the ruptured PAMPS chains still remained in DN gels in the form of crosslinking points for the PAAm chains. These newly formed crosslinking points enlarged the field of affected PAAm chain layers during crack propagation, which resulted in a large Γ_0 value for the prestretched DN gels. To describe the thickness of the affected PAAm layers in the intrinsic field, we propose a new feature size l_0, which is expressed as

$$l_0 = \left(2|i|_{max}+1\right)\left(\sqrt{n_{AAm}}\,l_{AAm}\right)\left(\phi_{PAAm}^{DN}\phi_{AAm}^{PAAm}\right)^{-\frac{1}{3}} \tag{24}$$

The value of l_0 of the DN gels in this study was calculated as 165 μm.

So far, we fully decomposed the fracture energy of the DN gels. The total fracture energy Γ was first decomposed into the intrinsic fracture energy Γ_0 and dissipated fracture energy Γ_d. Γ_d was further decomposed into the pre-yield dissipated fracture energy $\Gamma_{d,P}$ and yield dissipated fracture energy $\Gamma_{d,Y}$. Γ_0 was simultaneously contributed by the two interpenetrating networks PAAm (Γ_0^{PAAm}) and PAMPS (Γ_0^{PAMPS}). In addition, we obtained the feature sizes of the damage zone at the macro- to microscale. At the macroscale, we first obtained the feature size of the dissipation zone $l_d \sim 8.5$ mm, which was decomposed into the feature sizes of the pre-yield zone ($l_{d,P} \sim$ 5.1 mm) and yield zone ($l_{d,Y} \sim 3.4$ mm). At the microscale, the feature size of the intrinsic field l_0 is approximately the thickness of thousands of polymer chain layers, $\sim$ 165 μm.

5. Discussion of feature size

Feature size is widely used to characterize the crack-tip field of soft materials, and is relevant to the fracture behavior of materials. By introducing feature sizes, the crack-tip field is divided into different regions according to their deformation states, which helps in understanding the underlying toughening mechanisms. For the fracture of soft materials, two length scales are widely used (Creton and Ciccotti, 2016; Long et al., 2021; Zheng et al., 2021): the elasto-adhesive length associated with elastic deformation near the crack tip, and the dissipative length (or fracto-cohesive length) related to the near-tip dissipation. We now compare these two length scales with the feature sizes obtained in this study.

The elasto-adhesive length is defined as Γ/E, where Γ is the fracture energy and E is the elastic modulus. The elasto-adhesive length represents the boundary between the nonlinear and linear elastic regions, within which the deformation of materials is dominated by nonlinearity. For large deformation materials with nonlinearity, E should be the initial modulus at small strain, where the material can be considered as linear elastic. According to our uniaxial tensile test (Fig. 1a), E is estimated as the slope of the stress–stretch curve within a 5% strain, which is 0.03 MPa. The Γ value is chosen as Γ_p, which is 3622 J /m^2 according to our tearing test. The obtained elasto-adhesive length is 121 mm, which is even larger than the size of DN gel specimens used in our study. This confliction indicates that the DN gel is a strongly nonlinear soft material, and the deformation of DN gels in the elastic region (Fig. 7) is actually nonlinear because the linear elastic region is too far away to reach.

The other length scale, the dissipative length, is defined as Γ/W_f, where Γ is the fracture energy and W_f is the work of extension to fracture. The dissipative length determines the size of the region within which the stress and strain are concentrated and dissipation occurs. According to our uniaxial tensile test, W_f is the area of the stress–stretch curve before the specimen ruptures, which is measured as 1730 kJ /m^3. The dissipative length is calculated as 2 mm for the DN gels used in our study, which is of the same order of magnitude as the feature size of the dissipation zone l_d ($\sim$ 8.5 mm) measured in our experiment. However, it should be noted that in the definition of the dissipative length, the dissipated energy density is assumed to be homogenous in the dissipation zone and taken as W_f. This assumption contradicts our tearing test result that the dissipated energy density varies along the direction perpendicular to the crack

surface instead of being constant within a certain field (Fig. 8c). The value of W_f (1730 kJ $/m^3$) is larger than the maximum dissipated energy density (723 kJ $/m^3$) measured in our experiment in the dissipation field (Fig. 8c). Therefore, the dissipation length Γ/W_f underestimates the feature size of the dissipation zone.

From the above discussion, the two length scales, Γ/E and Γ/W_f, have disadvantages in describing the crack-tip field of DN gels. The Γ/E length scale is unsuitable for strongly nonlinear materials such as DN gels, and cannot provide practical guidance for their use. The Γ/W_f length scale is convenient to use but not very accurate in predicting the size of the dissipation zone because of the homogeneous stress assumption. Moreover, these two length scales are insufficient to describe the complex material behavior in the crack-tip field of DN gels. Therefore, more precise and comprehensive feature sizes are required.

Based on our extensive experiments and theoretical analysis, we obtained all the feature sizes in the damage zone of DN gels ranging from the macroscale to the microscale. The feature size of the dissipation zone l_d is 8.5 mm, which can be further decomposed into the feature size of the pre-yield zone ($l_{d,P} \sim 5.1$ mm) and yield zone ($l_{d,Y} \sim 3.4$ mm). The feature size of the intrinsic field l_0 is ~ 165 μm. These feature sizes have clear physical meanings and are closely related to the deformation states of the crack-tip field of DN gels. Our feature sizes establish a relationship between the deformation states of the crack-tip field and the fracture energy as well as provide new insights into toughening mechanisms.

6. Concluding remarks

In this study, we elucidated several contradictions related to the fracture of DN gels in previous studies, and characterized the fracture toughness and damage zone of DN gels by quantitatively decomposing the fracture energy and feature sizes. Combining the tearing and tensile test results, we divided the crack-tip field into four regions according to their deformation states: elastic, pre-yield, yield, and intrinsic fields. In addition, we developed an intrinsic fracture model by considering the complex interactions between the two interpenetrating networks in DN gels. Based on the experimental results and theoretical model, the contribution of the damage zone to the total toughness along with their feature sizes were determined.

It is worth mentioning that, several interesting phenomena were observed in our experiments. (i) The intrinsic fracture energy and dissipated fracture energy measured by our method are of the same order of magnitude, which contradicts the conventional understanding that the fracture energy of DN gels is dominated by the dissipated fracture energy. (ii) By measuring the fracture energy of prestretched DN gels, we found that the intrinsic fracture energy is dependent on the historical deformation instead of being a material constant. These two phenomena were explained by our intrinsic fracture model.

In summary, this study established a quantitative framework for decomposing the fracture toughness and feature sizes of the crack-tip field, which provides important insights into the underlying toughening mechanism of DN gels. The proposed quantitative framework could be generalized to characterize other soft materials with various toughening mechanisms, and to facilitate the design and application of future soft materials.

Authorship contributions

Yetong Jia: experiment work, the theory deriving and manuscript writing.
Zidi Zhou: experiment work, the theory deriving and manuscript writing.
Huilong Jiang: experiment work.
Zishun Liu: designing project, editing manuscript and project supervision.

Declaration of Competing Interest

The authors declare that they have no known competing financial interests or personal relationships that could have appeared to influence the work reported in this paper.

Data Availability

Data will be made available on request.

Acknowledgements

This work was supported by the National Natural Science Foundation of China [grant numbers 11820101001, 12172273].

Supplementary materials

Supplementary material associated with this article can be found, in the online version, at doi:10.1016/j.jmps.2022.105090.

References

Bai, R., Chen, B., Yang, J., Suo, Z., 2019. Tearing a hydrogel of complex rheology. J. Mech. Phys. Solids 125, 749–761.

Brown, H.R., 2007. A model of the fracture of double network gels. Macromolecules 40, 3815–3818.

Creton, C., Ciccotti, M., 2016. Fracture and adhesion of soft materials: a review. Rep. Prog. Phys. 79, 046601.

Fukao, K., Nakajima, T., Nonoyama, T., Kurokawa, T., Kawai, T., Gong, J.P., 2020. Effect of relative strength of two networks on the internal fracture process of double network hydrogels as revealed by in situ small-angle X-ray scattering. Macromolecules 53, 1154–1163.

Gent, A.N., 1974. Fracture mechanics of adhesive bonds. Rubber Chem. Technol. 47, 202–212.

Gent, A.N., Hamed, G.R., 1977. Peel mechanics of adhesive joints. Polymer Eng. Sci. 17, 462–466.

Gong, J.P., 2010. Why are double network hydrogels so tough? Eur. Phys. J. E Soft. Matter. 6, 2583.

Gong, J.P., Katsuyama, Y., Kurokawa, T., Osada, Y., 2003. Double-network hydrogels with extremely high mechanical strength. Adv. Mater. 15, 1155–1158.

Greensmith, H.W., 1963. Rupture of rubber. X. The change in stored energy on making a small cut in a test piece held in simple extension. J. Appl. Polym. Sci. 7, 993–1002.

Huang, R., Zheng, S., Liu, Z., Ng, T.Y., 2020. Recent advances of the constitutive models of smart materials — hydrogels and shape memory polymers. Int. J. Appl. Mech. 12, 2050014.

Lake, G.J., Thomas, A.G., Tabor, D., 1967. The strength of highly elastic materials. Proc. R Soc. Lond. A Math. Phys. Sci. 300, 108–119.

Lei, J., Li, Z., Xu, S., Liu, Z., 2021. A mesoscopic network mechanics method to reproduce the large deformation and fracture process of cross-linked elastomers. J. Mech. Phys. Solids, 104599.

Li, C., Wang, Z., Wang, Y., He, Q., Long, R., Cai, S., 2021. Effects of network structures on the fracture of hydrogel. Extreme Mech. Lett. 49, 101495.

Li, J., Wong, W.-Y., Tao, X.-m., 2020. Recent advances in soft functional materials: preparation, functions and applications. Nanoscale 12, 1281–1306.

Liang, S., Wu, Z.L., Hu, J., Kurokawa, T., Yu, Q.M., Gong, J.P., 2011. Direct observation on the surface fracture of ultrathin film double-network hydrogels. Macromolecules 44, 3016–3020.

Lin, S., Zhao, X., 2020. Fracture of polymer networks with diverse topological defects. Phys. Rev. E 102.

Liu, X., Liu, J., Lin, S., Zhao, X., 2020. Hydrogel machines. Mater. Today 36, 102–124.

Liu, Z., Toh, W., Ng, T., 2015. Advances in mechanics of soft materials: a review of large deformation behavior of hydrogels. Int. J. Appl. Mech. 735, 35.

Long, R., Hui, C.-Y., Gong, J.P., Bouchbinder, E., 2021. The fracture of highly deformable soft materials: a tale of two length scales. Annu. Rev. Condens. Matter Phys. 12, 71–94.

Long, R., Hui, C.Y., 2016. Fracture toughness of hydrogels: measurement and interpretation. Eur. Phys. J. E Soft. Matter. 12, 8069–8086.

Matsuda, T., Kawakami, R., Nakajima, T., Gong, J.P., 2020. Crack tip field of a double-network gel: visualization of covalent bond scission through mechanoradical polymerization. Macromolecules 53, 8787–8795.

Matsuda, T., Kawakami, R., Nakajima, T., Hane, Y., Gong, J.P., 2021. Revisiting the origins of the fracture energy of tough double-network hydrogels with quantitative mechanochemical characterization of the damage zone. Macromolecules 54, 10331–10339.

McCracken, J.M., Donovan, B.R., White, T.J., 2020. Materials as machines. Adv. Mater. 32, 1906564.

Nakajima, T., Kurokawa, T., Ahmed, S., Wu, W.-L., Gong, J.P., 2013. Characterization of internal fracture process of double network hydrogels under uniaxial elongation. Eur. Phys. J. E Soft. Matter. 9, 1955–1966.

Rivlin, R.S., 1953. Rupture of rubber. i. characteristic energy for tearing. J. Polym. Sci. 10, 291–318.

Seiffert, S., 2017. Origin of nanostructural inhomogeneity in polymer-network gels. Polym. Chem. 8, 4472–4487.

Tanaka, Y., 2007. A local damage model for anomalous high toughness of double-network gels. Europhys. Lett. 78.

Tang, J., Li, J., Vlassak, J.J., Suo, Z., 2017. Fatigue fracture of hydrogels. Extreme Mech. Lett. 10, 24–31.

Xu, S., Liu, Z., 2020. Coupled theory for transient responses of conductive hydrogels with multi-stimuli. J. Mech. Phys. Solids 143, 104055.

Yang, C., Suo, Z., 2018. Hydrogel ionotronics. Nat. Rev. Mater. 3, 125–142.

Yu, Q.M., Tanaka, Y., Furukawa, H., Kurokawa, T., Gong, J.P., 2009. Direct observation of damage zone around crack tips in double-network gels. Macromolecules 42, 3852–3855.

Zhang, T., Lin, S., Yuk, H., Zhao, X., 2015. Predicting fracture energies and crack-tip fields of soft tough materials. Extreme Mech. Lett. 4, 1–8.

Zhang, W., Liu, X., Wang, J., Tang, J., Hu, J., Lu, T., Suo, Z., 2018. Fatigue of double-network hydrogels. Eng. Fract. Mech. 187, 74–93.

Zhao, X., 2014. Multi-scale multi-mechanism design of tough hydrogels: building dissipation into stretchy networks. Eur. Phys. J. E Soft. Matter. 10, 672–687.

Zhao, X., Chen, X., Yuk, H., Lin, S., Liu, X., Parada, G., 2021. Soft materials by design: unconventional polymer networks give extreme properties. Chem. Rev. 121, 4309–4372.

Zheng, Y., Matsuda, T., Nakajima, T., Cui, W., Zhang, Y., Hui, C.Y., Kurokawa, T., Gong, J.P., 2021. How chain dynamics affects crack initiation in double-network gels. Proc. Natl. Acad. Sci. U S A 118.